Title	Measurement of input-impedance of helical type delay line
Sub Title	
Author	藤田, 広一(Fujita, Hiroichi) 柏木, 寛(Kashiwagi, Hiroshi)
Publisher	慶応義塾大学藤原記念工学部
Publication year	1965
Jtitle	Proceedings of the Fujihara Memorial Faculty of Engineering Keio University (慶応義塾大学藤原記念工学部研究報告). Vol.18, No.69 (1965.) ,p.25(1)- 41(17)
JaLC DOI	
Abstract	The characteristic impedance of traveling wave tube is characterized by the ratio of the square of the electric field to the power. But in this paper, the input impedance of helix defined as the ratio of the voltage to the current is considered and measured. This impedance plays a major role in the matching of helical type delay lines. The input impedance of helix has been analyzed in our previous paper. But the measurements for it, are not so easy that the experimental researches are very rare, because of their poor reproducibility and large errors. The mean diameter of the helix used in the measurement is 4.0mm, and values of the ratio of the conductor diameter to the pitch are between 2 to 5. Frequencies for the measurement are in the 4000 Mc band, and the measuring apparatus are all of the coaxial type. In order to prevent the axial component of the electric field of the helix from being disturbed, the diameter of the outer cylindrical conductor is chosen to be more than three times as large as that of the helix. The input impedance of the helix is much larger than the impedance of a coaxial type standing wave detector. Accordingly it is possible to make the standing wave ratio smaller by using an impedance transformer. The results of experiments show that the real part of the input impedance decreases with increased frequency, and its imaginary part has the same characteristics as those of the real part but are negative in value. The polarity of the imaginary part obtained by experiments coincides with that theoretically obtained through equivalent analysis for the distribution line, while in its frequency characteristics no coincidence is observed between the two. The tendency of the experimental values coincides with that of the theoretical ones. Experiments show that the measurement has a good reproducibility of its results, the maximum error for the real part being within 15 percent. This data is useful in designing the junction between a waveguide and a traveling wave tube, which will be discussed in the next report.
Notes	
Genre	Departmental Bulletin Paper
URL	https://koara.lib.keio.ac.jp/xoonips/modules/xoonips/detail.php?koara_id=KO50001004-00180069-0001

Measurement of Input-Impedance of Helical Type Delay Line

(Received June 2, 1965)

Hiroichi FUJITA*

Hiroshi KASHIWAGI**

Abstract

The characteristic impedance of traveling wave tube is characterized by the ratio of the square of the electric field to the power. But in this paper, the input impedance of helix defined as the ratio of the voltage to the current is considered and measured. This impedance plays a major role in the matching of helical type delay lines. The input impedance of helix has been analyzed in our previous paper. But the measurements for it, are not so easy that the experimental researches are very rare, because of their poor reproducibility and large errors. The mean diameter of the helix used in the measurement is 4.0mm, and values of the ratio of the conductor diameter to the pitch are between 2 to 5. Frequencies for the measurement are in the 4000 Mc band, and the measuring apparatus are all of the coaxial type. In order to prevent the axial component of the electric field of the helix from being disturbed, the diameter of the outer cylindrical conductor is chosen to be more than three times as large as that of the helix. The input impedance of the helix is much larger than the impedance of a coaxial type standing wave detector. Accordingly it is possible to make the standing wave ratio smaller by using an impedance transformer. The results of experiments show that the real part of the input impedance decreases with increased frequency, and its imaginary part has the same characteristics as those of the real part but are negative in value. The polarity of the imaginary part obtained by experiments coincides with that theoretically obtained through equivalent analysis for the distribution line, while in its frequency characteristics no coincidence is observed between the two. The tendency of the experimental values coincides with that of the theoretical ones. Experiments show that the measurement has a good reproducibility of its results, the maximum error for the real part being within 15 percent. This data is useful in designing the junction between a waveguide and a traveling wave tube, which will be discussed in the next report.

*藤 田 広 一, 助教授 Associate Professor, Faculty of Engineering, Keio University, Koganei-shi, Tokyo, Japan.

**柏 木 寛, 電気試験所所員 Electro Technical Laboratory, Tanahsi-machi, Kitatama-gun, Tokyo, Japan.

I. Introduction

Two physically significant parameters of the traveling wave tube are the power flow in the circuit and the electric field associated with it which acts on the electron stream. The ratio of the square of the electric field to the power can be evaluated by physical measurement even when it cannot be calculated. These parameters are used by C. Cuttler and J. R. Piece.[1] In this paper, however, the input-impedance of the helices are evaluated by experiments, and then compared with the result of our theoretical analysis of the delay circuits.[2]

The definition for the input impedance of the helix is the ratio of the voltage to the current at the input terminal. Using this definition, the equivalent circuit is composed easily, when the helix is connected to the other circuits, for instance, coaxial line, wave guide etc.. The difficulties of analysis of the helix end is caused by the unsymmetric distribution of the mutual inductances and capacitances.

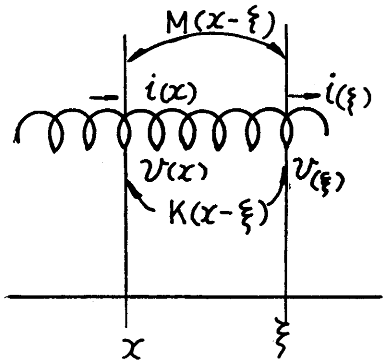

Fig. 1. Voltage and current distribution on the helix.

In Fig. 1, it is assumed that the voltage and the current on the helix are $v(x)$, $i(x)$ at the point x, $v(\xi)$, $i(\xi)$ at the point ξ and affects each other between two points by mutual inductance and capacitance. Then referring to Fig. 1, one can accordingly write the equations

$$-\frac{\partial v(x)}{\partial x}=\int_0^{\infty} L(x-\xi)\frac{\partial i(\xi)}{\partial t}d\xi\,, \tag{1}$$

$$-\frac{\partial i(x)}{\partial x}=C(x)\frac{\partial v(x)}{\partial t}+\int_0^{\infty} K(x-\xi)\frac{\partial\{v(x)-v(\xi)\}}{\partial t}d\xi\,, \tag{2}$$

where $L(x-\xi)$ is the mutual inductance between point x and point ξ, $K(x-\xi)$ is the capacitance between x and point ξ, $C(x)$ is the self capacitance at point x,

$v(x)$, $i(x)$ are voltage and current at point x,

$v(\xi)$, $i(\xi)$ are voltage and current at point ξ.

1) J. R. Pierce; Traveling-Wave Tubes, D. Van. Nostrand Co., Inc., New York N. Y.; 1950.

2) H. Fujita, H. Kashiwagi; Theoretical Study of the Electromagnetic Wave Propagation and Termination Concerning the Helical Type Delay Line, Proc. of the Fujihara Memorial Faculty of Erg., Keio Univ. Tokyo, JAPAN Vol. 15, No. 56, 1962, pp. 1~11.

Now, it is assumed that the voltage and current varies sinusoidally $e^{j\omega t}$. The distributions of the mutual inductance $L(x-\xi)$ and the capacitance $K(x-\xi)$ are as follows :

$$L(x-\xi)=L_0e^{-a|x-\xi|},$$
$$K(x-\xi)=K_0e^{-b|x-\xi|}.$$

The distribution of self capacitance is given by

$$C(x)=C_0+D(x),$$

whare, $$D(x)=D_0e^{-qx}.$$

The following result is obtained by substituting these assumptions into fundamental equations and by Laplace transformation,

$$z_{in}=\lim_{x\to 0} v(x)/i(x)=\sqrt{\eta-\omega^2\xi^2}-j\omega\xi, \tag{3}$$

where, $$\xi=\frac{L_0}{2(C_0+D_0)}\left\{\frac{C_0}{a^2}+\frac{D_0}{a(a+q)}-\frac{2K_0}{b(a^2-b^2)}\right\}$$

$$\eta=\frac{L_0}{C_0+D_0}\left\{1+\frac{1}{a}\right\}$$

For comparing the experimental results with the theoretical values, the input impedance of the helices are measured by using a coaxial type standing wave detector. In this case, the load impedance z_L is given by

$$z_L=\frac{\rho-j\tan\frac{2\pi}{\lambda_g}\cdot x_{\max}}{1-j\rho\tan\frac{2\pi}{\lambda_g}\cdot x_{\max}}\cdot z_0, \tag{4}$$

where z_0 is the characteristic impedance of the measuring system, ρ is the voltage standing wave ratio, $x_{\max}$ is the length from the load to the maximum point of the voltage standing waves, and λ_g is the guide wavelength.

Measurable values in Eq. (4) are ρ, $x_{\max}$ and λ_g. Comparing characteristic impedance to input impedance z_{in}, when the difference between two is extremely large, ρ takes inaccurate values. Usually, the double minimum method is used for high VSWR but in this experiment, an impedance transformer is used, for reason of its simplicity and accuracy. The impedance transformer is designed to have a standing wave ratio from 1.5 to 5.0.

II. Design of the impedance transformer

When designing an impedance transformer between two lines with different impedances, generally $1/4\cdot\lambda$ length line is used, where the line is terminated by the load $z_b=r+jx$. If a length from the generator to the reference plane is l, the input impedance is given by

$$z=R_0\left(\frac{z_L+R_0\tanh\gamma l}{R_0+z_L\tanh\gamma l}\right), \tag{5}$$

where γ is the propagation constant. If it is a lossless line, the propagation constant γ is equal to $j\beta$. Then Eq (5) is as follows:

$$z=R\left[\frac{r/R_0\left\{\cot^2\left(\frac{\pi}{2}\frac{\lambda_{g0}}{\lambda_g}\right)+1\right\}+j\left[x/R_0\cdot\left\{\cot^2\left(\frac{\pi}{2}\cdot\frac{\lambda_{g0}}{\lambda_g}\right)-1\right\}\right.}{\left\{\cot\left(\frac{\pi}{2}\cdot\frac{\lambda_{g0}}{\lambda_g}\right)-x/R_0\right\}^2+(r/R_0)^2}\right.$$
$$\left.\frac{\left.+\left\{1-(x/R_0)^2-(r/R_0)^2\right\}\cot\frac{\pi}{2}\frac{\lambda_{g0}}{\lambda_g}\right]}{}\right], \tag{6}$$

where the wavelength of the center frequency and the wavelengths of the optional frequencies are λ_{g0} and λ_g respectively. The length of the transformer is $l=1/4\cdot\lambda_{g0}$,

than $\quad \beta l=\frac{2\pi}{\lambda_g}\frac{\lambda_{g0}}{4}=\frac{\pi}{2}\cdot\frac{\lambda_{g0}}{\lambda_g}$ (7)

For the particular case, in which the load has no reactive component and when the frequency is equal to the center frequency, $x=0$, $\cot\left(\frac{\pi}{2}\cdot\frac{\lambda_{g0}}{\lambda_g}\right)=0$. Substituting them into Eq. (6), the following relation is obtained

$$z=R_0^2/r \tag{8}$$

When the load is pure resistance, the impedance transformer which has a characteristic impedance R_0 and length of $1/4\cdot\lambda_g$ placed between z and r. The efficiency of the transmission should be maximum.[3] On the other hand, if the load has the imaginary part and the frequencies are varied, z is very complicated, but the difficulty to calculate such impedance is overcome by use of the Smith Chart. This will be explained later.

Design plan is as follows:

1) The complete system has the same diameter for the outer cylinder, 19.2 mm, and transformation of the impedance depends only on the diameter of the inner cylinder.

2) The center frequency is 4,000 Mc. The real part of the input impedance of the helix is 500 Ω theoretically. It is extremely larger than the imaginary part. Therefore it is considered that the value of imaginary part is negligible.

3) The diameter of inner conductors are defined by

$$z_0=\frac{138}{\sqrt{\varepsilon}}\log_{10}b/a, \tag{9}$$

where a and b are the diameters of the inner and outer conductors respectively,

3) H. Nukiyama; Electromagnetism, Maruzen Co., Inc., Tokyo, JAPAN, 1962.

and ε is the dielectric constant of the medium. From Eq. (9), $b/a=13.99$ is obtained, then the diameter of the inner conductor in the transformer is $a=1.37$ mm and its length is $\lambda_{g0}/4=18.8$ mm.

III. Method of support of the helix and its termination

For the reliability and reproducibility of experiments, the supporting method of the helix is very importance. Various supporting methods were considered, but in this case the helix is placed on two parallel quartz rods, and the ends are supported by a Teflon piece as shown in Fig. 2. To prevent the reflecting power from the helix end, some resistive materials are used.

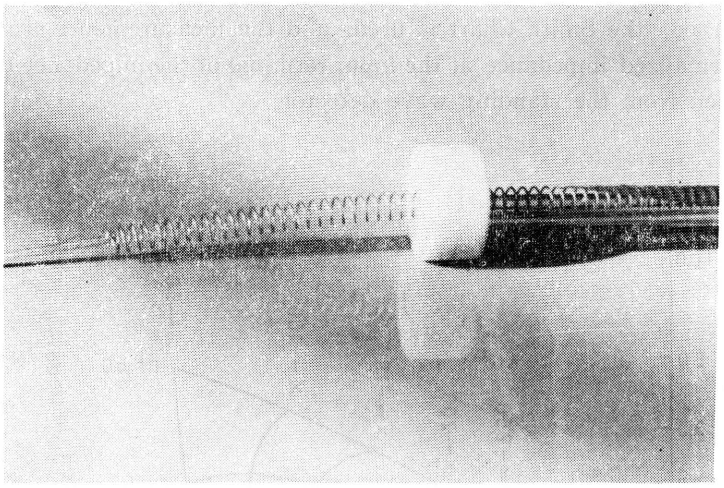

Fig. 2. Supporting method of the helix.

IV. Measuring system

The measuring system is shown in Fig. 3. The klystron 2K54 is used as the microwave source and is modulated by 1kc square wave. Output power is adjusted

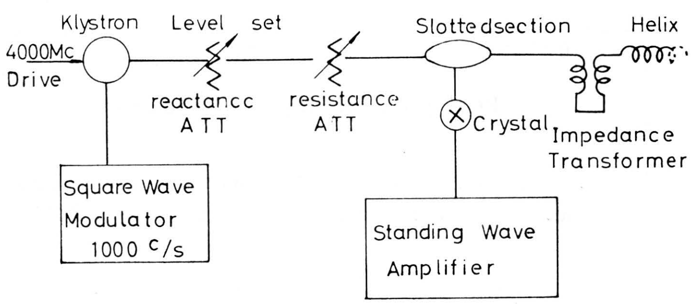

Fig. 3. Block diagrams of Measuring apparatus.

by a reactance attenuator. The microwave power is supplied to the helix through the coaxial type standing wave detector and impedance transformer. The reflections from the helix end and other equipment are so small that they are negligible, then the reflected power is only from the input terminal of the helix.

V. Measuring method (I)

Two methods are considered: One is the method obtained from the relation of Eq. (8). It is represented by the relation of the normalized impedance at the input terminal of the trasfomer to the load impedance, then the calculating values of Eq. (8), Table 1, and the transfering chart, Fig. 4, 5, 6, 7, and 8 are obtained. This method is more accurate than the other method but not so practical. In the other practical method, the Smith Chart is used, and the measurements are performed by this. Normalized impedance at the input terminal of the impedance transformer z_{NA} is obtained from the standing wave detector.

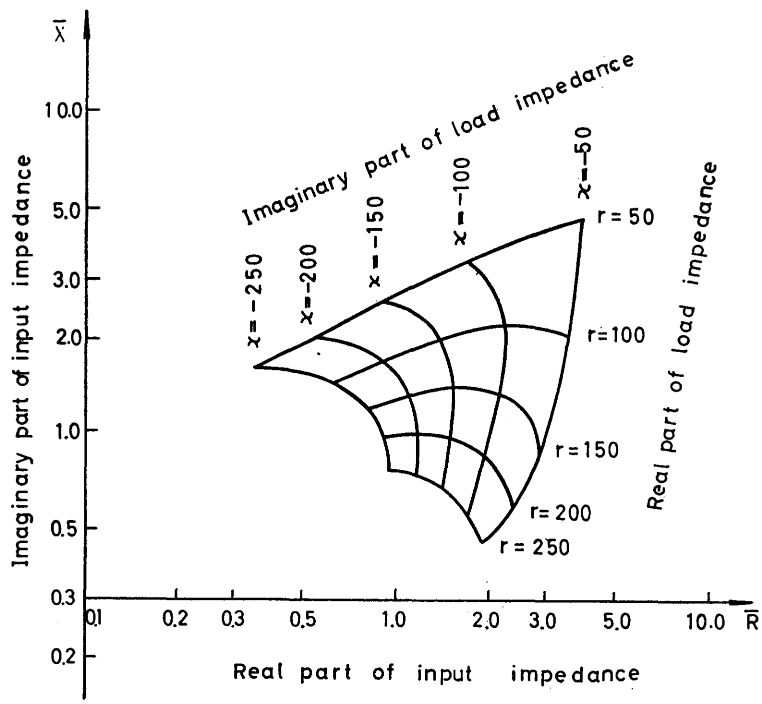

Fig. 4. Plots of normalized input impedance vs. load impedance at the entrance of the transformer. Frequency $f=3,800$ Mc. [ref. eq. (8)]

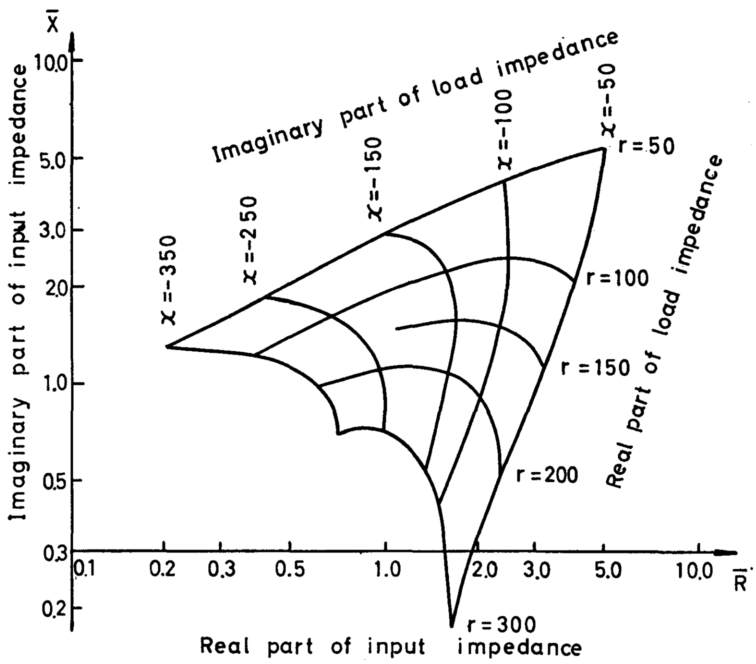

Fig. 5. The case of the frequency 3,900 Mc.

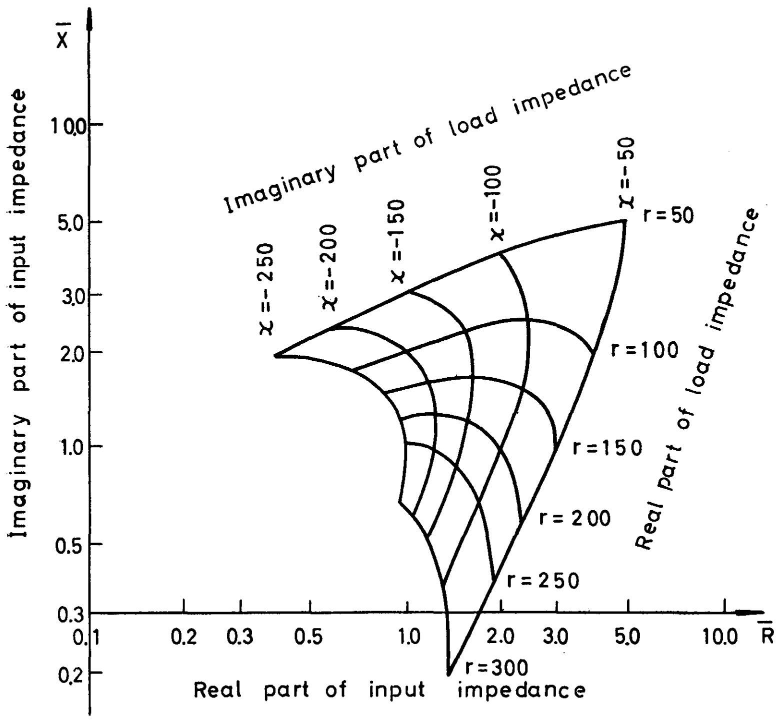

Fig. 6. The case of the frequency 4,000 Mc.

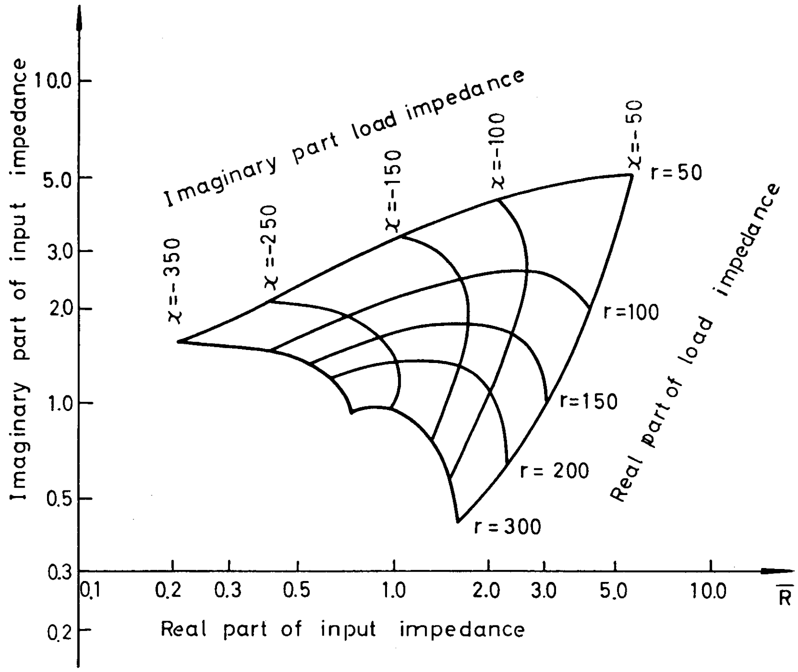

Fig. 7. The case of the frequency 4,100 Mc.

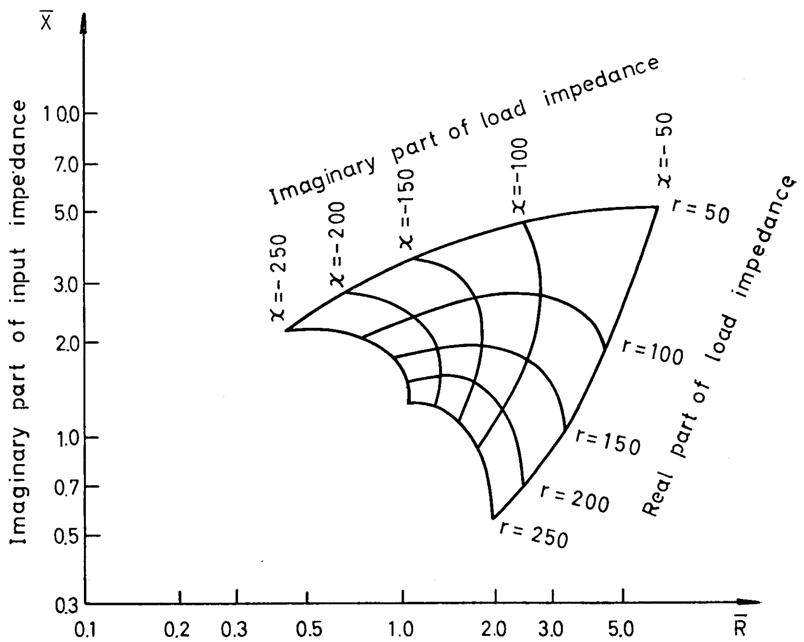

Fig. 8. The case of the frequency 4,200 Mc.

Table 1. Calculating value of Eq. (8).

I

3800 Me/s			
$r(\Omega)$	$x(\Omega)$	$\bar{R}$	$\bar{X}$
50	−50	3.932	4.661
100		3.620	2.012
150		2.859	0.941
200		2.292	0.467
250		1.894	0.448
50	−100	1.661	3.487
100		2.222	2.249
150		2.147	1.361
200		1.911	0.826
250		1.674	0.504
50	−150	0.871	2.580
100		1.383	1.997
150		1.544	1.423
200		1.516	0.999
250		1.415	0.670
50	−200	0.528	1.995
100		0.913	1.690
150		1.116	1.231
200		1.182	1.007
250		1.168	0.744
50	−250	0.353	1.601
100		0.638	1.425
150		0.826	1.196
200		0.924	0.964
250		0.957	0.756

II

3900 Me/s			
$r(\Omega)$	$x(\Omega)$	$\bar{R}$	$\bar{X}$
50	−50	4.987	5.472
100		4.000	2.119
200		2.355	0.536
300		1.623	0.179
50	−150	0.999	2.991
100		1.538	2.273
200		1.600	1.123
300		1.334	0.569
50	−250	0.385	1.842
100		0.690	1.639
200		0.976	1.123
300		0.984	0.569
50	−350	0.200	1.298
100		0.378	1.217
200		0.616	0.970
300		0.706	0.712
100	−100	2.499	2.524
150		2.308	1.507
200		2.001	0.938
300		1.501	0.406
150	−50	3.001	0.998
	−150	1.661	1.608

III

4000 Me/s			
$r(\Omega)$	$x(\Omega)$	$\bar{R}$	$\bar{X}$
50	−50	5.000	5.000
100		4.000	2.000
150		3.000	1.000
200		2.353	0.588
250		1.923	0.385
50	−100	2.00	4.00
100		2.50	2.50
150		2.35	1.47
200		2.00	1.00
250		1.724	0.690
50	−150	1.000	3.000
100		1.538	2.308
150		1.667	1.667
200		1.600	1.200
250		1.470	0.882
50	−200	0.588	2.353
100		1.000	2.000
150		1.200	1.600
200		1.250	1.250
250		1.219	0.976
50	−250	0.385	1.923
100		0.690	1.724
150		0.882	1.470
200		0.976	1.219
250		1.000	1.000
350	−50	1.400	0.200
	−100	1.321	0.377
	−200	1.007	0.615

IV

4100 Mc/s			
$r(\Omega)$	$x(\Omega)$	$\bar{R}$	$\bar{X}$
50	−50	5.668	5.088
100		4.202	1.964
150		3.007	1.002
200		2.389	0.647
300		1.634	0.363
50	−100	2.216	4.282
100		2.664	2.623
150		2.400	1.625
200		2.053	1.087
300		1.521	0.600
50	−150	1.040	3.231
100		1.633	2.472
150		1.740	1.792
200		1.651	1.311
300		1.358	0.775
50	−250	0.404	2.096
100		0.721	1.883
150		0.917	1.614
200		1.007	1.352
300		1.005	0.941
50	−350	0.207	1.551
100		0.391	1.467
150		0.534	1.348
200		0.633	1.212
300		0.722	0.951

V

4200 Mc/s			
$r(\Omega)$	$x(\Omega)$	R	$\bar{X}$
50	−50	6.42	5.06
100		4.40	1.90
150		3.16	1.038
200		2.42	0.705
250		1.96	0.544
50	−100	2.47	4.58
100		2.85	2.74
150		2.50	1.71
200		2.11	1.17
250		1.792	0.08
50	−150	1.074	3.479
100		1.739	2.641
150		1.822	1.920
200		1.708	1.423
250		1.545	1.099
50	−200	0.668	2.753
100		1.114	2.338
150		1.309	1.885
200		1.338	1.504
250		1.288	1.215
50	−250	0.427	2.277
100		0.757	2.048
150		0.956	1.763
200		1.044	1.488
250		1.057	1.254

$$\bar{R}+j\bar{X}=\frac{R+jX}{50\,\Omega}$$

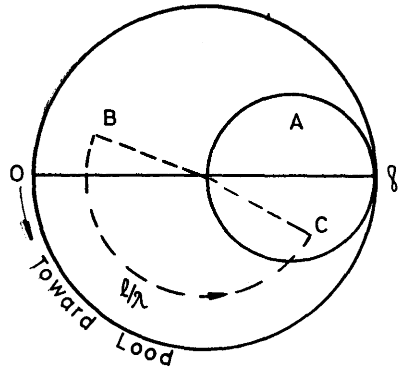

Fig. 9. Transfering method on the Smith Chart.

When z_{NA} is point A in Fig. 9,

$$z_{NA}=R_{NA}+jX_{NA} \tag{10}$$

is assumed where the suffix N indicates the normalized value. The characteristic impedance of the standing wave detector is z_0, and the characteristic impedance of the impedance transformer is R_0, therefore the impedance at the entrance of the impedance transformer z_{NB} is as follows:

$$z_{NB}=\frac{z_0}{R_0}(R_{NA}+jX_{NA})\,. \tag{11}$$

This is point B on the Smith Chart.

The input impedance of the helix is given by rotating z_{NB} along curve B toward the load by the length l/λ_g, then it is point C on the Smith Chart and assumed as follows:

$$z_{NC}=R_{NC}+jX_{NC}\,. \tag{12}$$

Hence the input impedance of the helix z_h is

$$z_h=R_0(R_{NC}+jX_{NC})\,. \tag{13}$$

VI. Measuring method (II)

……Setting up the equivalent reference plane……

It is important problem to set up the reference plane for measuring the impedance. Usually the geometrical reference plane does not coincide with the practical one. In this paper, the latter is used. In Fig. 10 where the short plate is placed on the plane $2-2'$, the input impedance from the plane $1-1'$ is

$$z_R=jR_0\tan\beta l\,, \tag{14}$$

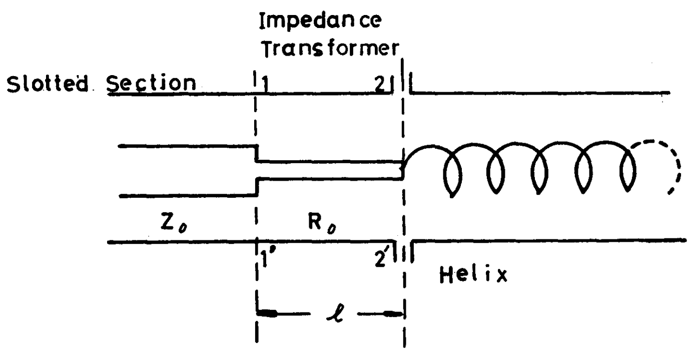

Fig. 10. Cross section of the measuring system.

where R_0 is the characteristic impedance of the transfomer (158.1 Ω), l is the length of the transformer ($l=\lambda_{4GC}/4=18.8$ mm). When the frequency is 4,000 Mc, z_R approach infinity, but at other frequencies is finite. Generally, the reflection coefficient Γ on the plane $1-1'$ in Fig. 10 is given by

$$\Gamma_R=|\Gamma_R|e^{j\varphi}=\frac{\dot{z}_R-\dot{z}_0}{\dot{z}_R+\dot{z}_0}=\frac{jR_0\tan\beta l-z_0}{jR_0\tan\beta l+z_0}$$
$$=\angle\exp j\left[\tan^{-1}\left(-\frac{R_0}{z_0}\tan\beta l\right)-\tan^{-1}\left(\frac{R_0}{z_0}\tan\beta l\right)\right], \tag{15}$$

where z_0 is the characteristic impedance ($z_0=50$ Ω) of the standing wave detector. The voltages on the line can be expressed in the following form:

$$V(x)=V_ie^{\gamma x}+V_re^{-\gamma x}, \tag{16}$$

where V_i is the incident voltages, V_r is the reflection voltages and $V(x)$ is the composed voltages.

Using reflection coefficient $\Gamma=\frac{V_r}{V_i}e^{-2\gamma x}=\Gamma_Re^{-2\gamma x}$ and $\gamma=j\beta$ to rewrite Eq. (16), the following relation is obtained,

$$V(x)=V_ie^{j\beta x}(1+\Gamma)=V_ie^{j\beta x}(1+\Gamma_Re^{-2j\beta x})$$
$$=V_ie^{j\beta x}(1+|\Gamma_R|e^{j(\varphi-2\beta x)}), \tag{17}$$

then

$$\left|\frac{V(x)}{V_i}\right|=1+|\Gamma_R|e^{j(\varphi-2\beta x)}. \tag{18}$$

Fig. 11. shows the vector diagram of the reflection coefficient and the phase from Eq. (18). $|V(x)/V_i|$ is the absolute value of the vector. When $e^{j(\varphi-2\beta x)}=1$, the value of $|V(x)/V_i|$ is maximum and $e^{j(\varphi-2\beta x)}=-1$, the value of it is minimum. Hence, if the distance x is satisfied the following relation

$$|\varphi-2\beta x|=n\pi \quad (n=0,\ 1,\ 2,\ \ldots\ldots)$$

then,

1) it has maximum value when n is an even number, or
2) it has minimum value when n is an odd number.

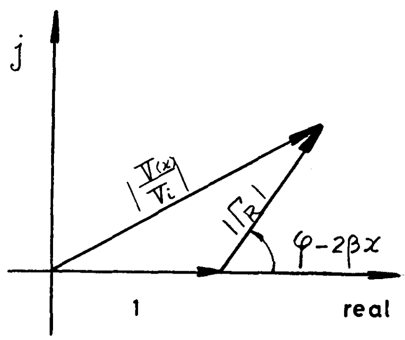

Fig. 11. The relation of the reflection coefficient and the phase.

When the probe is moved toward the generator, it is decided from n that the first extremum is maximum or minimum when

$$1^\circ\quad \varphi\geqq 0,\quad \begin{cases}\varphi<\pi,\ \varphi-2\beta x=0,\ \to\ \text{max.},\\ \varphi>\pi,\ \varphi-2\beta x=\pi,\ \to\ \text{min.},\end{cases}$$

$$2^\circ \quad \varphi \leqq 0, \quad \begin{cases} |\varphi| < \pi, & |\varphi - 2\beta x| = \pi, \rightarrow \text{min.}, \\ |\varphi| > \pi, & |\varphi - 2\beta x| = 2\pi, \rightarrow \text{max.}. \end{cases}$$

From Eq. (15) and (18) l_{min} is obtained theoretically. In the practical frequency band, 3,700～4,300 Mc, the measured values of l_{min} are shown in Table 2.

Table 2. Relation of the length of minimum point to frequencies.

Freq. (Mc)	3,700	3,800	3,900	4,000	4,100	4,200	4,300
φ (°)	4.3	2.8	1.4	0	−1.4	−2.8	−4.3
l_{min} (mm)	20.76	20.04	19.38	18.75	18.16	17.58	17.03

In practical cases, it is necessary to use the correction of $\Delta L = L - l_{min}$.

VII. The result

The sizes of helices that have been used for experiment are as follows (ref. Fig. 12).

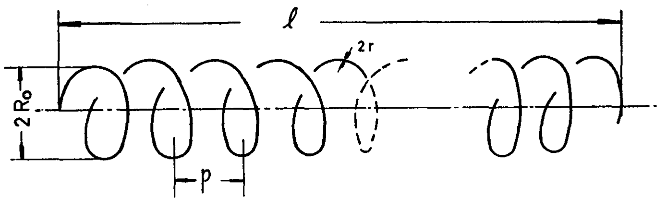

Fig. 12. Notations for the helix.

Mean diameter of the helix $2R_0 = 4.0$ mm,
mean diameter of the wire $2r = 0.4$ mm,
piches $p = 0$ 8, 1.2, 1.6, 2.0 mm,
the length of the helix $l \simeq 150$ mm.

The frequency range is from 3.700 to 4,300 Mc, and measuring system is shown in Fig. 13.

For 1.6 mm pitch, the processes for obtaining load impedance are illustrated in Fig. 13.

1. It is necessary to measure the VSWR, ρ, and valtage minimum points. If the value of standing wave detector scale was x_0, the distance from this point to reference plane is as follows:

$$x_{min} = x_0 - L + l_{min},$$

where L is the length of standing wave detector.

2. Using the value of ρ, x_{min}, point A on the Smith Chart, the input terminal of impedance transformer is obtained. (ref. Fig. 13)

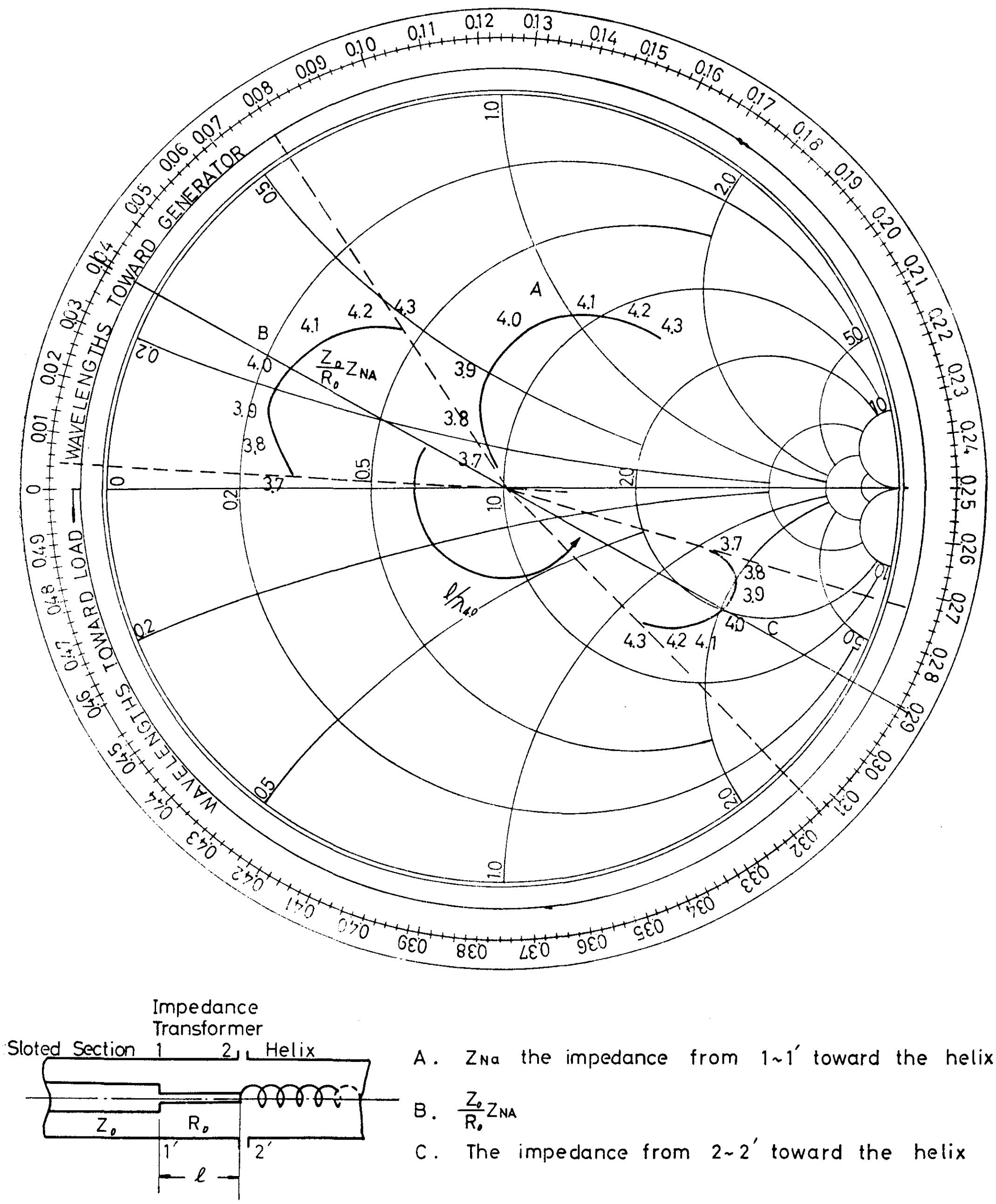

Fig. 13. Typical input inpedance characteristics of a 3.7~4.3 kMc. [pitch p=1.6 mm]
(Mean diameter of the helix : 4.0 mmϕ
Mean diameter of the conductor : 0.4 mmϕ)

3. If the value of point A was $R_{NA}+jX_{NA}$ normalized impedance in the transformer is given by

$$z_{NB}=\frac{z_0}{R_0}\left(R_{NA}+jX_{NA}\right).$$

This is a point B on the Smith Chart.

4. Rotating point B toward the load by the length l/λ, where λ is the wave-length of the measuring frequency, l is the length of the impedance transformer (75/4 mm), the input impedance at the plane $2-2'$ is obtained by the point C. This is the normalized input impedance of the helix.

5. If the value of point C was R_L+jX_L, the input impedance of the helix z_h is as follows:

$$z_h=R_0(R_L+jX_L)$$

The input impedance of the helices on each pitch are shown in Fig. 14 and 15 with frequency characteristcs. The impedance characteristic is as follows:

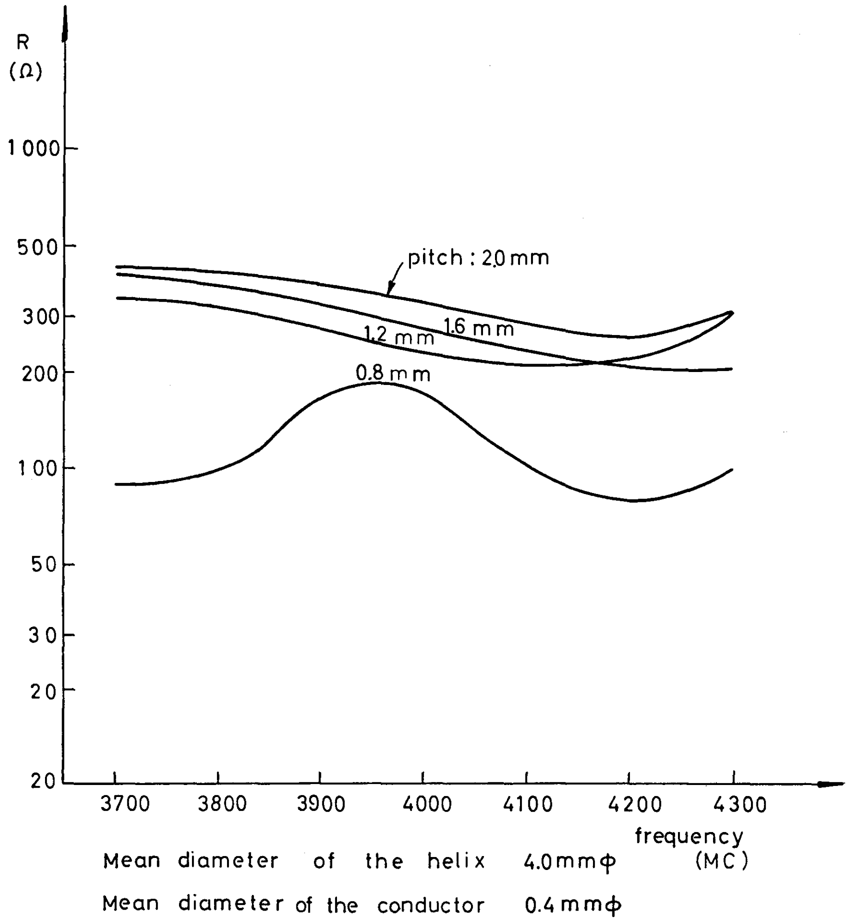

Fig. 14. The frequency characteristics of the real parts of helices input impedance $(R-jX)$.

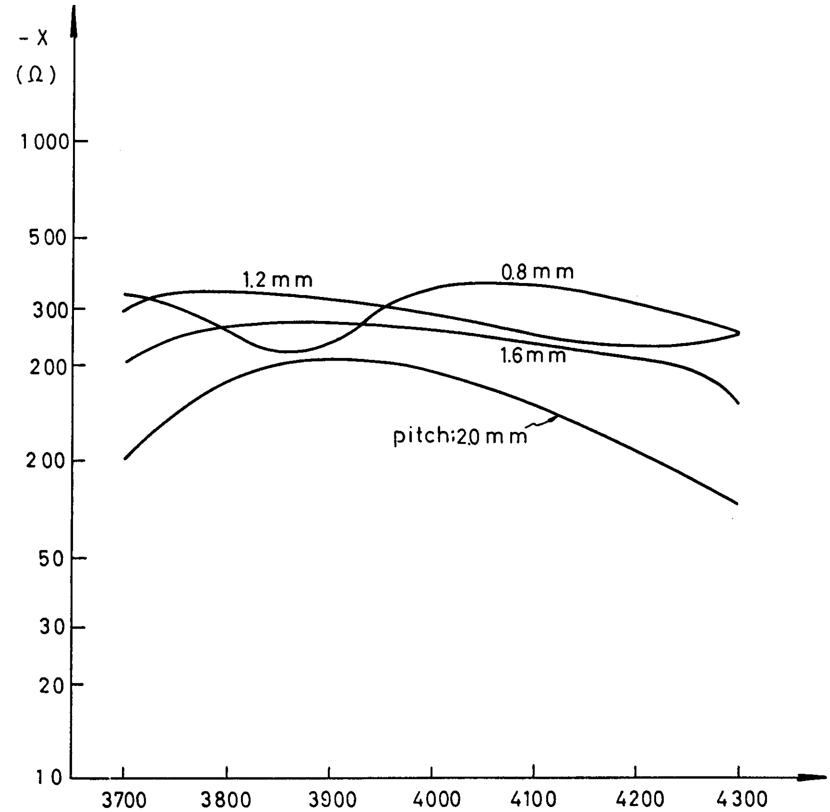

Mean diameter of the helix 4.0 mφ

Mean diameter of the conductor 0.4 mφ

Fig. 15. The frequency characteristics of the imaginary part of helices input impedance ($R-jX$).

i) The real part increases from 80 Ω to 500 Ω with increasing pitch and its value decreases from 430 Ω to 210 Ω with frequency when the pitch is small, for instance, 0.8 mm or at upper limit of oscillation 4,300 Mc, the data has considerable error.

ii) The imaginary part decreases gradually from 400 Ω to 100 Ω with increasing pitch and decreases with increasing frequency. The case in which the pitch is 0.8 mm and frequency is 4,300 Mc is the same as i).

VIII. Discussion

As shown in Fig. 16, the curve of the 0.8 mm pitch helix is quite apart from any other curves. This is caused by the large load impedance and mechanical

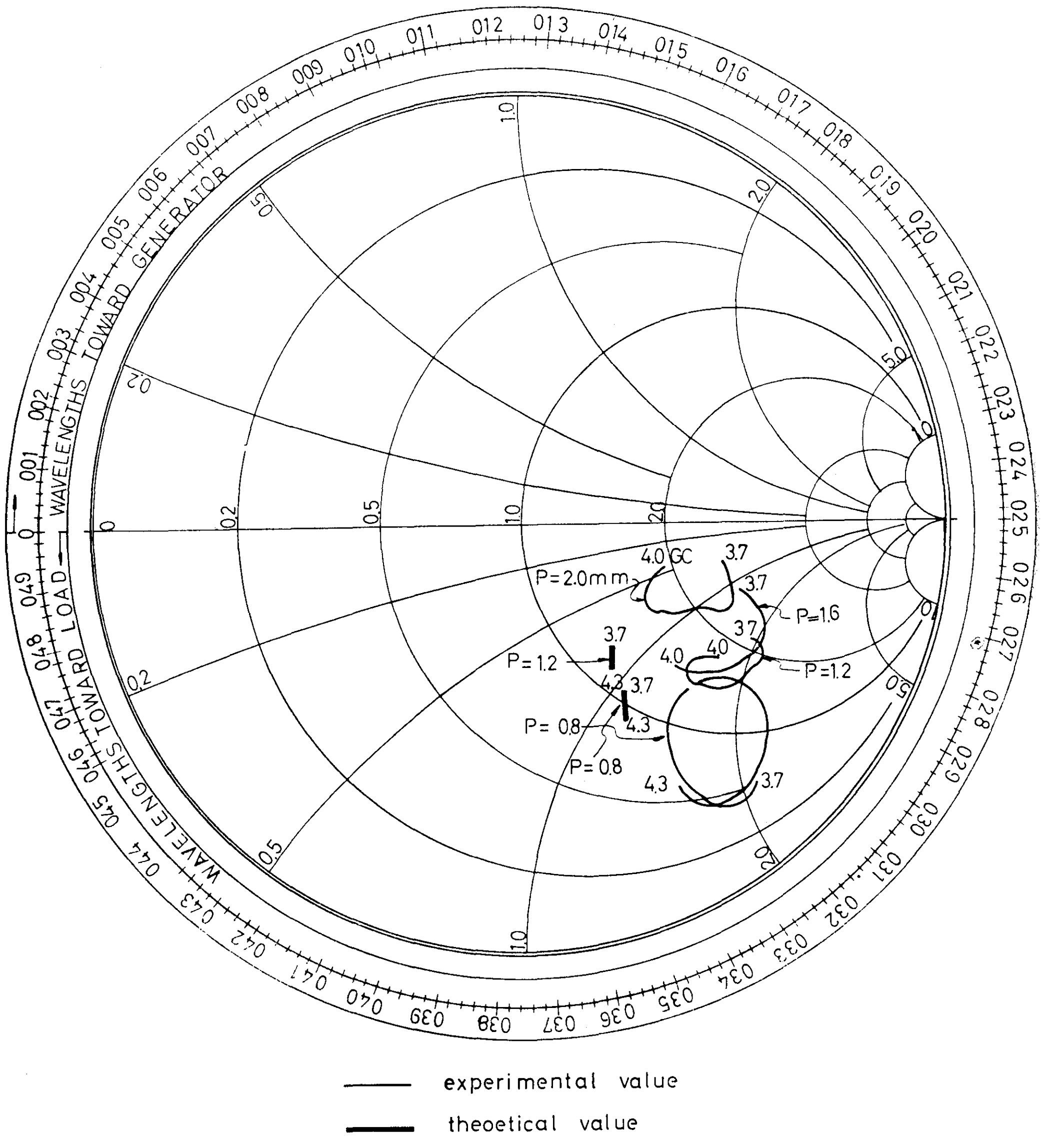

Fig. 16. Comparison of the theoretical values and experimental value.

error. The error at 4,300 Mc is caused by the distorted pattern arising in the impedance transformer. The error in the measured value is due to the read out error of the minimum point of the standing wave pattern. If the read out error was ± 0.5 mm, the error of wave number δ on the Smith Chart is as follows:

$$\frac{0.1}{\lambda_{3.7GC}} \leqq \delta \leqq \frac{0.1}{\lambda_{4.3GC}}.$$

Hence,

$$0.0123 \leqq \delta \leqq 0.0144 .$$

Fig. 16 shows the theoretical curves of helix impedance. It is assumed that q and D_0 are proportional to self inductance and self capacitance. When the pitch is less than 1.2 mm, the measured impedance coincides with theoretical values.

IX. Conclusion

It is possible to obtain stable and accurate values when the helix input impedance are measured. The tendency of the experimental value coincides with the theoretical value, but it is necessary to discuss the various parameters in detail. The real parts of the input impedance decrease in proportion to the frequency and are proportional to the pitch. The imaginary parts of the input impedance decrease in proportion to the frequecy, their signs are negative, and the absolute value decreases with increasing pitch length.

Acknowledgement

The authors would like to express their appreciation to Dr. H. Nukiyama for profitable discussions regarding this work and Mr. Uji who assisted them with many instrumentation problems. Thanks also go to Mr. R. Fukuhara and Mr. T. Okazaki for their assistance in laboratory measurements.